Available online at www.sciencedirect.com
SCIENCE DIRECT®
Physics of the Earth and Planetary Interiors 136 (2003) 3–9
PHYSICS OF THE EARTH AND PLANETARY INTERIORS
www.elsevier.com/locate/pepi

Flow-law for ringwoodite at subduction zone conditions

Yaqin Xu [a], Donald J. Weidner [a,*], Jiuhua Chen [a], Michael T. Vaughan [a], Yanbin Wang [b], Takeyuki Uchida [b]

[a] *Geosciences Department, Center for High Pressure Research, SUNY at Stony Brook, Stony Brook, NY 11794, USA*
[b] *Consortium for Advance Radiation Sources, The University of Chicago, Chicago, IL 60439, USA*

Received 12 October 2001; received in revised form 22 March 2002; accepted 22 August 2002

Abstract

The plastic properties of ringwoodite, a high-pressure modification of olivine, are experimentally determined at the pressure of 20 GPa and temperatures up to 1350 °C. Stress relaxation experiments have been carried out on fine-grained samples using a two-stage T-cup multiple anvil high-pressure apparatus with synchrotron-generated X-rays. We observe the presence of a significant weakening of the shear strength with a decrease from 2.5 to 0.2 GPa between 600 and 1000 °C. In this region, the activation energy, *U*, is about 275 kJ/mol and it decreases with increasing stress, reaching a value of about 200 kJ/mol when the shear stress attains 2.5 GPa. We propose that the plasticity is associated with vigorous dislocation glide controlled by short-range lattice resistance forces. At lower temperatures, the shear strength is mildly dependent on temperature reaching 3 GPa at room temperature, while above 1000 °C, the flow may be governed by a power-law relation with *n* about 3.5.

Keywords: Rheology; Ringwoodite; Subduction zone; Flow properties; Transition zone

1. Introduction

Ringwoodite is generally expected to be the most abundant mineral in the earth for the depth range of 550–660 km. Forming the lower half of the transition zone, the ringwoodite layer plays a pivotal role in mantle dynamics, making the plastic properties of ringwoodite important constraints on the flow of material in this part of the mantle. In regions of subduction zones, the ringwoodite stability field hosts high levels of seismicity, including some of the earth's greatest events such as the 1994 Bolivian earthquake (Silver et al., 1995). Two processes vie for the mechanism of deep faulting. One involves the metastable transformation of olivine to ringwoodite throughout the region where ringwoodite is the stable phase (Green and Burnley, 1989; Griggs and Baker, 1968; Kirby et al., 1996). In this model the transformation is kinetically inhibited by the low temperatures, and the transformation process results in faulting. The second mechanism is a plastic-instability process in which the material begins to deform plastically, heats up, the higher temperature induces softening which further localizes the flow and concentrates more heating (Hobbs and Ord, 1988; Ogawa, 1987). This process may end in melting or it may terminate simply with high flow rates in a plastic media. The plastic-instability process requires that the strength be strongly temperature dependent. Needed to further our understanding of all of these processes is a quantitative model of the plastic flow-laws for ringwoodite at the pressure, temperature, and stress levels that act in these various regions. However, such fundamental parameters have never been measured at

* Corresponding author. Tel.: +1-631-632-8241.
E-mail address: dweidner@sunysb.edu (D.J. Weidner).

0031-9201/03/$ – see front matter © 2003 Elsevier Science B.V. All rights reserved.
doi:10.1016/S0031-9201(03)00026-8

the appropriate conditions. A major challenge for rheological studies is how to measure strain/stress at such high pressures and high temperatures. Here we exploit the stress/strain metrics derived from X-ray studies. Since a high-energy synchrotron X-ray beam is able to penetrate thick ceramic pressure media, the strain/stress in the sample can be measured in situ by analyzing diffraction peak-broadening (Weidner et al., 1998). This newly developed high-pressure technology with the aid of the synchrotron allows us to acquire rheological properties of mantle minerals throughout the *P–T* range of the upper mantle. Here we report quantitative flow-laws and investigate the deformation mechanisms at high pressures and temperatures up to 20 GPa and 1350 °C. Our data span a range of strain rate from 10^{-5} to 10^{-7} s^{-1}. This is typical of laboratory experiments, but is, of course, much faster than the mantle flow processes. Earthquakes, however, are very fast events, and the earthquake process will include deformation that is both faster and slower than those of these experiments. In like fashion, the stresses during the earthquake process in the rupturing media are expected to be in the range of stresses studied here (a few GPa) as even the deep Bolivian event demonstrated an average stress drop—which is measured for the entire affected region—of 0.1 GPa.

2. Experimental details

The polycrystalline ringwoodite sample was synthesized from a fine powder of San Carlos olivine at 19 GPa and 1300 °C for 2 h using the multi-anvil 2000 t uniaxial split-sphere apparatus (USSA-2000) at the Stony Brook High Pressure Laboratory. X-ray diffraction demonstrated that the San Carlos olivine was fully transformed to ringwoodite with no impurity phases observed in the sample.

A two-stage T-cup high-pressure apparatus with eight tungsten carbide second-stage cubes each with 2 mm truncations (Vaughan et al., 1998) was used to generate high pressure up to 20 GPa for the stress relaxation experiment. The pressure medium for the cell assembly is a boron-epoxy octahedron. The pressure in the sample was measured in situ by the analysis of the X-ray diffraction pattern from NaCl. A disk-type heater was made from the rhenium foil with a $LaCrO_3$ insulator. The temperature in this cell can reach 2000 °C and was monitored by a thermocouple during the experiment.

In this study, the deviatoric stress is heterogeneous within the X-ray scattering volume and is manifested as a strain-broadening of the diffraction peaks (Cullity, 1978; Weidner, 1998; Weidner et al., 1992,1994a,b,c,1998). The deviatoric stress is generated as the sample is pressurized owing to elastic heterogeneity and anisotropy within the powdered sample. Ringwoodite powders with a mean grain size of <5 μm were directly loaded into the sample chamber and hydrostatically cold-compressed to a high pressure of 20 GPa at room temperature and then heated to a high temperature for the stress relaxation. We kept the pressure relatively constant during heating. This microscopic strain, determined from peak-broadening, is elastic strain. The microscopic elastic stress σ in the lattice is determined by multiplying the Young's modulus by the elastic strain ε. The Young's modulus of ringwoodite used in this study is taken to be

$$E = 295 + 3.7P - 0.0569T$$

where P is the pressure (GPa), T the temperature (°C), and E is given in GPa (Weidner et al., 1984; Meng et al., 1993; Jackson et al., 2000; Sinogeikin et al., 1998). The resolution of the shear stress is about 0.2 GPa. Since total strain does not change with time, the plastic strain rate is simply the negative of the elastic strain rate. Taken together, these results yield both stress and strain rate as a function of the environmental conditions.

These are relaxation experiments with all of the attendant limitations of this style of measurement. Steady state is difficult to demonstrate. Weidner et al. (2001) demonstrate that the stress/strain rate values obtained by this method agree very well with those derived from the models of Frost and Ashby (1982) for spinel and corundum. Their models are based mostly on the indentation method for the region of comparison. Indeed, the method described here is very similar to the indentation method, where the material is 'self'-indented and the stress/strain relation is measured with X-ray methods. The big advantage here is that a much broader range of experimental environments can be interrogated. In this study, the uncertainties in the results come mostly from the limitations of the physical model. The

uncertainty of pressure, temperature, or Young's modulus will contribute a few percent to the final result. The model, however, could be several percent. The only confirmation of the model effects must come from comparisons with existing data such as suggested previously. In such comparisons, we generally find good agreement within 10–20% of the absolute values for stress.

3. Experimental results

In these experiments, we followed two distinct pressure–temperature–time paths. In the first, illustrated in Fig. 1, the ringwoodite sample in the pressure chamber is compressed to 20 GPa at room temperature, then the decay of stress with time t is monitored as the temperature is increased in distinct steps. Below 600 °C, stress relaxation is relatively slow with a strain rate $<10^{-7}\,s^{-1}$. Above 600 °C, the stress first drops rapidly within 20 min corresponding to a strain rate higher than $10^{-5}\,s^{-1}$, then the stress relaxes more slowly with a strain rate $<10^{-7}\,s^{-1}$. However, the stress never stops dropping and will, presumably, approach to zero if the time is long enough. Strength is a useful concept even within the plastic flow regime; it expresses the amount of stress that the solid can support for very long times (or at very low strain rates). The 3000 s strength, or the maximum shear stress that the sample can support after more than 3000 s relaxation at which the strain rate is less than about $10^{-7}\,s^{-1}$, is illustrated in Fig. 2. These data are very straightforward and are robust. The 3000 s strength measured at different temperatures for five samples with different heating paths are illustrated here and are sensitive to temperature, but are relatively insensitive to the heating history of the sample. Below 600 °C, the shear strength decreases slowly with temperature, beginning at about 3 GPa at room temperature. Between 600 and 1000 °C, the strength decreases dramatically from 2 to 0.2 GPa; between 1000 and 1350 °C, the strength is nearly a constant value of 0.2 GPa, which is very close to the detection limit.

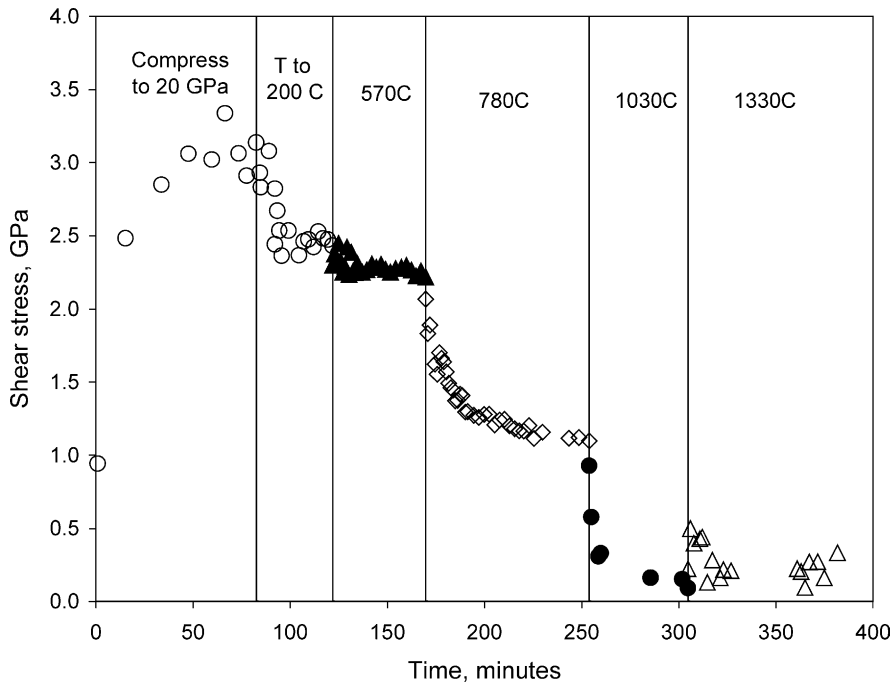

Fig. 1. Shear stress in sample during experiment. Initially as the sample is loaded to 20 GPa of pressure at room temperature, the shear stress increases elastically and then saturates as yielding occurs. As temperature is increased to 200 °C little relaxation of the shear stress occurs. Temperature is thereafter illustrated as a function of time during which the temperature is raised in steps.

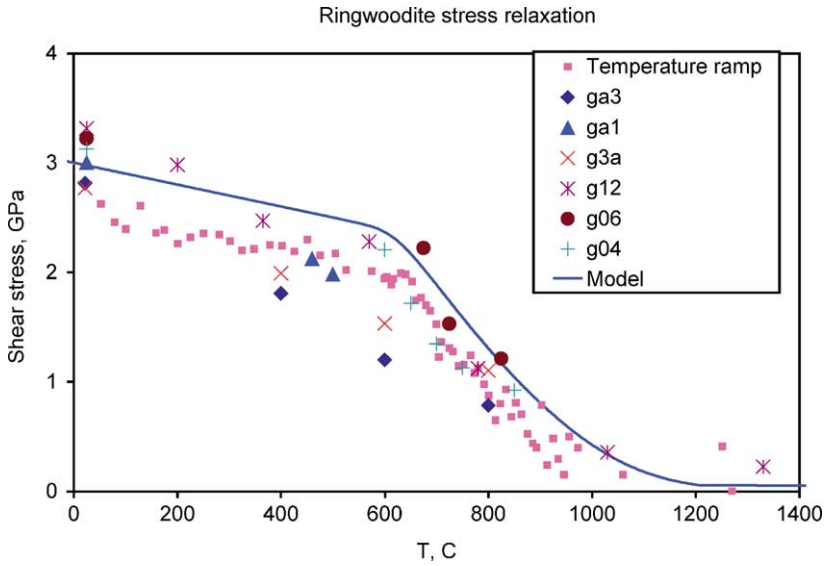

Fig. 2. 3000 s strength as a function of temperature. The shear stress supported by the sample from different experiments after the first 3000 s is illustrated as a function of temperature. Each symbol given in the caption represents a different experimental run. The runs that begin with the letter 'g' are experiments where temperature is increased in steps and held constant for a period of time. The experiment defined by 'Temperature ramp' is for an experiment where the temperature is gradually increased as a function of time. The solid line illustrates the shear stress given by the model described in the Eq. (3).

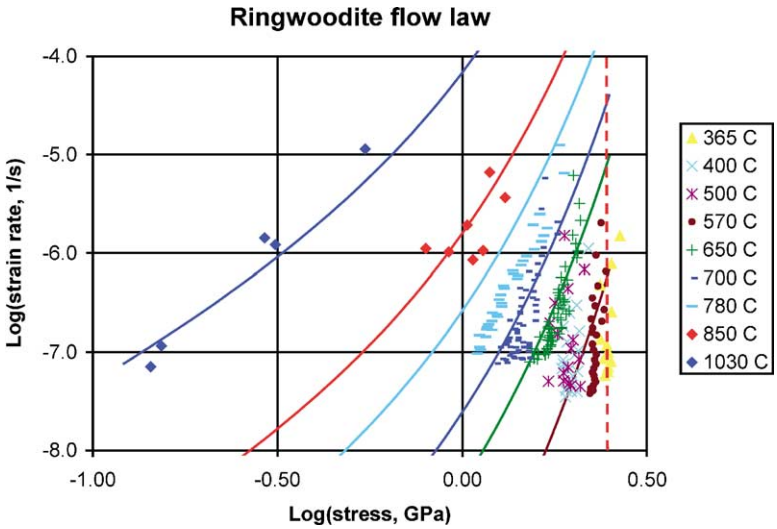

Fig. 3. Flow-law of ringwoodite. Symbols represent inferred stress and strain rate for different temperatures. These data represent several experimental runs of the type illustrated in Fig. 1. The vertical line represents the low temperature strength (3 GPa) while the curves reflect the relationships given by the model of Eq. (3).

The second style of experimental path is to increase temperature at a constant slow rate during the entire experiment (1 °C/min). These data are also illustrated in Fig. 2 and show an identical weakening/instability process throughout this temperature range.

As in the classic relaxation experiment, where total strain is maintained as constant, the measurement of elastic strain with time suffices to yield both stress and strain rates (Poirier, 1985). Stress is simply obtained by multiplying the elastic strain by an elastic modulus. The elastic strain rate is equal to the negative of the plastic strain rate. The first style of data can be easily expressed as stress/strain rate and several experimental runs are represented as such in Fig. 3. Since the sample always enters a new temperature regime from one with higher stresses and significant plastic yielding, it is justified to assume that new dislocations need not be generated for 'equilibrium' flow. We fit parametric models to these data assuming that they are at least a quasi-steady state relationship.

We choose a few possible parameterizations of the flow-law. The general form is given as

$$\dot{\varepsilon} = A\left(\frac{\sigma}{\mu}\right)^{n} \exp\left[\frac{-U(\sigma)}{RT}\right] \quad (1)$$

where A is the pre-exponential constant, R the gas constant, n the stress exponent, $U(\sigma)$ the activation energy which may be a function of the stress σ, and μ the shear modulus.

The values of n and of the stress dependence of the activation energy depend on the mechanism responsible for deformation. The case where activation energy is independent of stress, that is power-law creep, typically yields n between 3 and 5. In this case all curves in Fig. 3 should be parallel with this slope. Only the highest temperature data, those at 1030 °C, with a slope of about 3.5, yield slopes <10 or so. We thus conclude that the deformation observed here is not in the power-law creep regime.

Dislocation glide that is thermal and stress driven is typically described with a value of $n = 2$ and an activation energy that is stress dependent such as

$$U(\sigma) = U_0\left(1 - \frac{\sigma/\mu}{\tau}\right) \quad (2)$$

where τ is a material constant related to the yield strength. The activation energy, which involves both τ and U_0 determines the spacing between the curves in Fig. 3, while τ defines the slope of the curves. The parameters τ and U_0, as well as the pre-exponential, A, of Eq. (1), were determined as

$$\dot{\varepsilon} = 5 \times 10^{9}\left(\frac{\sigma}{\mu}\right)^{2} \exp\left\{\frac{275}{RT}\left(1 - \frac{\sigma/\mu}{0.075}\right)\right\} \quad (3)$$

to optimize the fit to the data in Figs. 2 and 3.

This model is used to calculate the stress as temperature is ramped and compared with the observations in Fig. 2 and is also used to calculate stress/strain rate relations and compared with the observations in Fig. 3. The model does accurately represent the observations between 600 and 1000 °C. For lower temperatures, we set the strength to a fixed value:

$$\sigma = 3.0 - Tb$$

where shear stress is given in GPa and T in °C. We used a value of $b = 0.001$ GPa/K.

4. Discussion

We proposed two deformation regimes and possibly a third can be classified in terms of the stress and temperature from these experiments. At high stress ($\sigma > 2$ GPa) and low temperature ($T < 600$ °C), stress relaxation is controlled by dislocation glide assisted solely by the effective stress and with little help from thermal energy since the temperature is too low for thermal activation of dislocation. This region is characterized by a high apparent stress exponent (>20), a low activation energy and insensitivity of strength to temperature and time. The shear strength in this region is relatively insensitive to temperature or strain rate and can be approximated by a constant of about 3 GPa. This strength is significantly lower than that of Meade and Jeanloz (1990) who found a room-temperature shear strength of about 8 GPa. They determined strength in a diamond anvil cell study that measured the pressure gradient with ruby fluorescence and the sample thickness after the experiment. A more recent diamond anvil study by Kavner deduced a room-temperature strength of about 3 GPa (Kavner and Duffy, 2001). This is in excellent agreement with our room-temperature results. Their study directly measures the deviatoric stress using side-entry X-rays and from the lattice spacings parallel and perpendicular to the principle stresses. Furthermore, the data

reported in this paper is consistent with similar data from a previous study that focused on comparing wet and dry samples (Chen et al., 1998).

At temperature above 600 °C, thermal energy assists glide activity in the sample. The flow mechanism for stress relaxation and for the weakening/instability of strength is associated with dislocation glide with a vigorous thermal activation of dislocation over short-range barriers, probably Perierls lattice resistance or short-range obstacles. The shear stress supported in the sample ranges from 0.2 to 2.0 GPa and the relaxation rate depends on temperature, time, and stress. The activation energy is strongly stress-dependent, which is anticipated by dislocation glide. The high apparent stress exponent of about 5–20, indicates that the power-law for dislocation climb is not active.

By 1000 °C, the effective power, n, of a power-law creep relation has decreased to 3.5. Yet, the strain rate at this temperature is compatible with the dislocation glide values for Eq. (3) deduced from lower temperature data. This suggests that this region is at the boundary between glide and climb. Higher temperature data, with high stress resolution is required to determine if this is indeed the onset of power-law creep, or whether power-law creep is yet a higher temperature phenomena at these stress levels.

These results provide constraints on models for deep focus earthquakes involving plastic instabilities. We find that below 600 °C, the rheology of ringwoodite resembles an ideal plastic material. The maximum shear stress that ringwoodite can support is about 3 GPa. Higher stresses are relaxed more quickly than our ability to observe them in the laboratory (faster than $10^{-3}\,s^{-1}$), yet lower stresses do not further relax at strain rates slower than the minimum that we observe in the laboratory ($10^{-7}\,s^{-1}$). Furthermore, the strength is almost independent of temperature. Such a region would not be capable of a plastic-instability that requires a strong temperature dependence of strength. We thus conclude that 600 °C marks the lower temperature bound for a plastic-instability in ringwoodite.

The high temperature limit for a plastic-instability mechanism of earthquakes can also be estimated with this data. If the sample has indeed reached the power-law creep regime at 1000 °C with $n = 3.5$ (which is consistent with our data but not required by our data), then obstacles will be overcome and the stress/strain rate relation should continue with no discontinuity to lower values of each. Extrapolating our curves along a power-law relation, we find that a shear stress of only 30 MPa will produce a flow rate $>10^{-11}\,s^{-1}$. Seismic activity produces a flow of $10^{-15}\,s^{-1}$ (Holt, 1995), considerably slower than this plastic flow. Thus, at these conditions, plastic flow will continue to decrease the stress below the stress drop levels observed seismically and bring a halt to earthquakes. Thus, the critical temperature regime for triggering a plastic-instability-type earthquake in a ringwoodite region is estimated to be 600–1000 °C. Above 1000 °C, we suggest that ringwoodite is too weak to sustain the stresses necessary to generate seismicity and below 600 °C it does not exhibit a temperature dependent strength that can give rise to an instability.

Acknowledgements

This work was supported by the National Science Foundation Grant EAR 9909266 and CHiPR Science and Technology Center Grant EAR 8920239. Synchrotron work was done at the National Synchrotron Light Source, Brookhaven Labs, and the Advanced Photon Source, Argonne Labs. The authors would like to thank Drs. Jerry Hastings and Mark Rivers for their support. This is MPI Publication 295.

References

Chen, J., Inoue, T., Weidner, D.J., Wu, Y., Vaughan, M.T., 1998. Strength and water weakening of mantle minerals, olivine, wadsleyite, and ringwoodite. Geophys. Res. Lett. 25, 575–578.

Cullity, B.D., 1978. Elements of X-Ray Diffraction. Addison-Wesley, New York, 287 pp.

Frost, H.J., Ashby, M.F., 1982. Deformation-Mechanism Maps: The Plasticity and Creep of Metals and Ceramics. Pergamon Press, Oxford, 166 pp.

Green, H.W., Burnley, P.C., 1989. A new self-organizing mechanism for deep-focus earthquakes. Nature 341, 733–737.

Griggs, D.T., Baker, D.W., 1968. The Origin of Deep-Focus Earthquakes: Properties of Matter Under Unusual Conditions. Wiley, New York, pp. 23–42.

Hobbs, B.E., Ord, A., 1988. Plastic instabilities: implications for the origin of intermediate and deep earthquakes. J. Geophys. Res. 93, 10521–10540.

Holt, W.E., 1995. Flow fields within the Tonga slab determined form the moment tensors of deep earthquakes. Geophys. Res. Lett. 22, 989–992.

Jackson, J.M., Sinogeikin, S.V., Bass, J.D., 2000. Sound velocities and elastic properties of gamma-Mg_2SiO_4 to 873 K by Brillouin spectroscopy. Am. Mineralogist 852, 296–303 (special issue dedicated to Orson L. Anderson).

Kavner, A., Duffy, T.S., 2001. Strength and elasticity of ringwoodite at upper mantle pressures. Geophys. Res. Lett. 28 (14), 2691–2694.

Kirby, S.H., Stein, S., Okal, E.A., Rubie, D.C., 1996. Metastable mantle phase transformations and deep earthquakes in subducting oceanic lithosphere. Rev. Geophys. 34, 261–306.

Meade, C., Jeanloz, R., 1990. The strength of mantle silicates at high pressures and room temperature: implications for the viscosity of the mantle. Nature 348, 533–535.

Meng, Y., et al., 1993. In situ *P–T* X-ray diffraction studies on three polymorphs (a, b, g) of Mg_2SiO_4. J. Geophys. Res. 98 (B12), 22199–22207.

Ogawa, M., 1987. Shear instability in a viscoelastic material as the cause of deep focus earthquakes. J. Geophys. Res. 92, 13801–13810.

Poirier, J.-P., 1985. Creep of Crystals: High-Temperature Deformation Processes in Metals, Ceramics and Minerals. Cambridge Earth Science Series. Cambridge University Press, Cambridge, 260 pp.

Silver, P.G., et al., 1995. Rupture characteristics of the deep Bolivian earthquake of 9 June 1994 and the mechanism of deep-focus earthquakes. Science 268, 69–73.

Sinogeikin, S.V., Katsura, T., Bass, J.D., 1998. Sound velocities and elastic properties of Fe-bearing wadsleyite and ringwoodite. J. Geophys. Res. B: Solid Earth Planets 103 (9), 20819–20825.

Vaughan, M.T., et al., 1998. T-cup: a new high-pressure apparatus for X-ray studies. Rev. High Press. Sci. Technol. 7, 1520–1522.

Weidner, D.J., 1998. Rheological studies at high pressure. In: Ribbe, P.H. (Ed.), Reviews in Mineralogy. Ultrahigh-Pressure Mineralogy: Physics and Chemistry of the Earth's Deep Interior. Mineralogical Society of America, Washington, DC, pp. 493–524.

Weidner, D.J., Sawamoto, H., Sasaki, S., Kumazawa, M., 1984. Single-crystal elastic properties of the spinel phase of Mg_2SiO_4. J. Geophys. Res. 89, 7852–7860.

Weidner, D.J., et al., 1992. Characterization of stress, pressure, and temperature in SAM85: a DIA type high pressure apparatus. In: Syono, Y., Manghnani, M.H. (Eds.), High-Pressure Research: Application to Earth and Planetary Sciences. American Geophysical Union, Washington, DC, pp. 13–17.

Weidner, D.J., Wang, Y., Vaughan, M.T., 1994a. Deviatoric stress measurements at high pressure and temperature. In: Schmidt, S.C., Shaner, J.W., Samara, G.A., Ross, M. (Eds.), Proceedings of the AIRAPT Conference on High-Pressure Science and Technology, 1993, pp. 1025–1028.

Weidner, D.J., Wang, Y., Vaughan, M.T., 1994b. Strength of diamond. Science 266, 419–422.

Weidner, D.J., Wang, Y., Vaughan, M.T., 1994c. Yield strength at high pressure and temperature. Geophys. Res. Lett. 21, 753–756.

Weidner, D.J., Wang, Y., Chen, G., Ando, J., 1998. Rheology measurements at high pressure and temperature. In: Manghnani, M.H., Yagi, T. (Eds.), Properties of Earth and Planetary Materials at High Pressure and Temperature. Geophysical Monograph. American Geophysical Union, Washington, DC, pp. 473–480.

Weidner, D.J., et al., 2001. Subduction zone rheology. Phys. Earth Planetary Interiors 127, 67–81.